Northern Lake Impacts on Local Seasonal Climate

Z. LONG AND W. PERRIE

Fisheries and Oceans Canada, Bedford Institute of Oceanography, Dartmouth, and Department of Engineering Math, Dalhousie University, Halifax, Nova Scotia, Canada

J. GYAKUM

McGill University, Montréal, Quebec, Canada

D. CAYA

Ouranos Consortium, and Université du Québec à Montréal, Montréal, Quebec, Canada

R. LAPRISE

Université du Québec à Montréal, Montréal, Quebec, Canada

(Manuscript received 31 January 2006, in final form 31 October 2006)

ABSTRACT

It is well known that large lakes can perturb local weather and climate through mesoscale circulations, for example, lake effects on storms and lake breezes, and the impacts on fluxes of heat, moisture, and momentum. However, for both large and small lakes, the importance of atmosphere–lake interactions in northern Canada is largely unknown. Here, the Canadian Regional Climate Model (CRCM) is used to simulate seasonal time scales for the Mackenzie River basin and northwest region of Canada, coupled to simulations of Great Bear and Great Slave Lakes using the Princeton Ocean Model (POM) to examine the interactions between large northern lakes and the atmosphere. The authors consider the lake impacts on the local water and energy cycles and on regional seasonal climate. Verification of model results is achieved with atmospheric sounding and surface flux data collected during the Canadian Global Energy and Water Cycle Experiment (GEWEX) program. The coupled atmosphere–lake model is shown to be able to successfully simulate the variation of surface heat fluxes and surface water temperatures and to give a good representation of the vertical profiles of water temperatures, the warming and cooling processes, and the lake responses to the seasonal and interannual variation of surface heat fluxes. These northern lakes can significantly influence the local water and energy cycles.

1. Introduction

Great Bear and Great Slave Lakes are two major lakes in the Mackenzie River basin (Figs. 1a,b). As large lakes, they perturb local climate through lake-effect storms, impacts on fluxes of heat, moisture, and momentum, and related mesoscale weather processes. Weather events can greatly influence the hydrodynamic regimes of lakes, for example, by surface layer mixing and upwelling, and in turn, weather events are affected through the large differences in heat capacity, roughness length, and albedo of water compared with nearby soil and vegetation, as well as differences in the vertical transfer of heat in the water column compared with those on land. Therefore, it is important to understand the atmosphere–lake interactions.

Previous studies suggest that the midlatitude lakes have significant impacts on local water and energy cycles (Bates et al. 1993; Hostetler et al. 1993; Bonan 1995; Lofgren 1997; Small and Sloan 1999). Inclusion of lakes significantly improves simulations of local temperature, evaporation, and precipitation compared to simulations that neglect the lake effects. For example, the presence of the Great Lakes results in a phase shift in the annual cycles of latent and sensible heat fluxes,

Corresponding author address: Dr. William Perrie, Bedford Institute of Oceanography, 1 Challenger Drive, P.O. Box 1006, Dartmouth, NS B2Y 4A2 Canada.
E-mail: perriew@dfo-mpo.gc.ca

DOI: 10.1175/JHM591.1

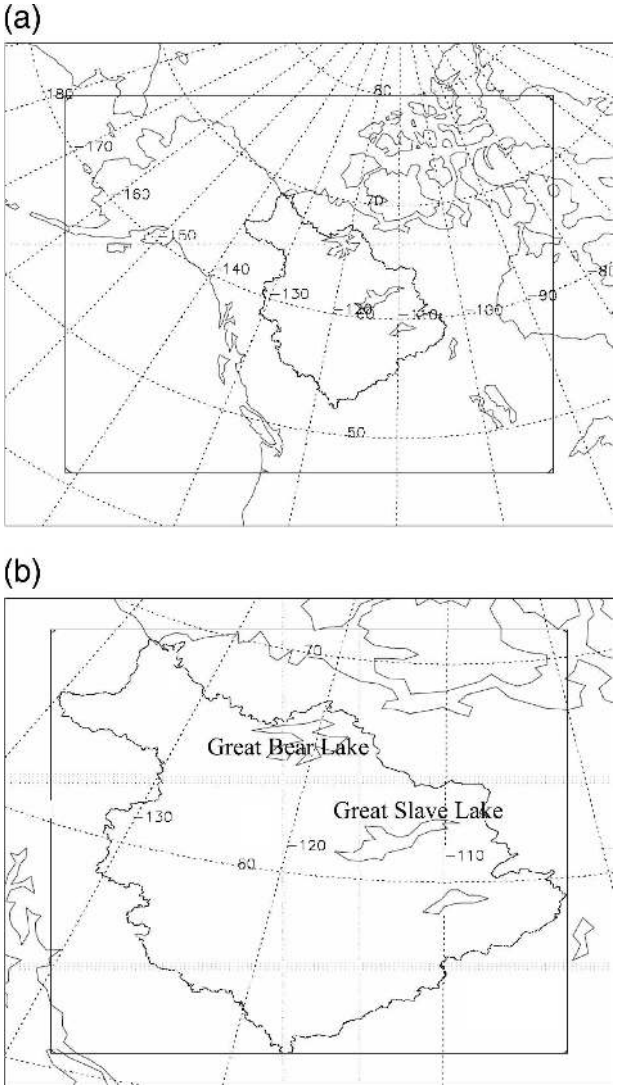

FIG. 1. (a) CRCM domain for the 51-km coarse-resolution grid, indicating the Mackenzie basin outline, and the nine-point lateral sponge zone. (b) Same as in Fig. 1a but showing the 15-km fine-resolution domain.

increases of the local evaporation and precipitation during the autumn and winter, and alters the meridional air temperature gradient (Lofgren 1997; Bates et al. 1993; Hostetler et al. 1993; Bonan 1995). While most atmosphere–lake studies have focused on the lower latitudes, particularly on the Great Lakes, the importance of atmosphere–lake interactions in northern Canada is largely unknown, for both large and small lakes.

Understanding atmosphere–lake interactions is a critical issue in studies of the water and energy cycles over the Mackenzie River basin (MRB) (Stewart et al. 1998; Rouse et al. 2003). Lakes occur in a wide variety of different sizes in the MRB and occupy 10% of the entire region (Rouse et al. 2003). The combined area of the two largest lakes, Great Bear Lake and Great Slave Lake, represents 3.3% of the total area of the MRB (Blanken et al. 2003). Located on the Arctic Circle, Great Bear Lake is the largest lake within the borders of Canada, with a surface area of 31 000 km^2 and a total volume of 2200 km^3. Great Bear Lake is deep, with a maximum recorded depth of 446 m in its central lake basin and an average depth of 72 m. Most of its water is in the vicinity of 4°–6°C, with the exception of shallow bays where the water temperatures can reach 17°C at the height of summer. In summer, this lake is isothermal, unstratified, and well mixed, with uniform temperatures even in its deepest areas. During summer wind storms, water from shallow lake zones, such as Smith Arm, Keith Arm, McVicar Arm, Dease Arm, and McTavish Arm, circulates and exchanges with water from the deeper areas (MacDonald et al. 2004).

Great Slave Lake is located between Great Bear Lake and Lake Athabasca. The surface area of Great Slave Lake is 27 200 km^2 with a total volume of 1070 km^3. This lake consists of a central basin, a northern arm, and an eastern arm called Christie Bay (Schertzer et al. 2003). It is the deepest lake in North America, with a maximum depth of 614 m (Blanken et al. 2003). The mean depth of the main lake, exclusive of the eastern arm, is estimated at 32 m from bathymetric data (Schertzer et al. 2003). Observations of the overlake meteorology and heat exchange in 1998 and 1999 were presented by Schertzer et al. (2003), Rouse et al. (2003), and Blanken et al. (2003).

Great Bear and Great Slave Lakes have large heat capacities and are capable of modifying the local water and energy cycles and thus constitute an important issue in the Canadian Global Energy and Water Cycle Experiment (GEWEX) Enhanced Study (CAGES; Stewart et al. 1998; Rouse et al. 2003). Observational evidence confirms the expected atmosphere–lake interactions between northern lakes and the surrounding regions. For example, Great Slave Lake is colder than the surrounding land in early summer after the final ice melts and warmer than the surrounding land in late fall and early winter before it freezes over. The difference in temperature between the middle of Great Slave Lake and the northern shore exhibits an approximate linear increase, from −6°C in June to 6°C in December. In summer, the lake receives a large net amount of solar radiation, but as the surface sensible heat and latent heat fluxes over the lake are small, most of the received solar radiation is used to heat the lake. In fall, the solar radiation is small, and the surface sensible and latent heat fluxes are the dominant components in the heat

exchange between the lake and the atmospheric boundary layer (Rouse et al. 2003). Although evaporation rates in summer are small, they increase significantly after August, with 85%–90% of the total evaporation occurring after mid-August (Rouse et al. 2003; Blanken et al. 2003). Therefore, these northern lakes act as energy sinks in the summer and as energy sources in the fall and introduce a large seasonal thermal lag into the regional climate (Rouse et al. 2003).

On longer time scales, observational evidence shows an interannual response of Great Slave Lake to atmospheric variations (Schertzer et al. 2003; Rouse et al. 2003). It is well known through in situ and satellite observations that ice breakup on Great Slave Lake typically precedes that on Great Bear Lake by about 1 month. Due to the relatively warm climatic conditions in the Mackenzie River basin coincident with the 1997/98 El Niño, the lake ice over Great Slave Lake melted several weeks earlier in 1998 than in 1999. This early thaw of lake ice greatly increased the absorption of solar radiation and thus influenced the lake water temperature. The average surface water temperature in 1998 was 3.5°C higher than in 1999 (Schertzer et al. 2003). Correspondingly, the total evaporation in 1998 exceeded that in 1999 by about 25% (Rouse et al. 2003; Blanken et al. 2003). Although most studies have focused on Great Slave Lake, these results are applicable to the other northern lakes, such as Great Bear Lake (Rouse et al. 2003; Blanken et al. 2003); this will be confirmed in this study.

In this study, the Princeton Ocean Model (POM) of Mellor (1998) is coupled to the Canadian Regional Climate Model (CRCM) of Caya and Laprise (1999) for Great Bear Lake and Great Slave Lake, as an attempt to examine the interaction between large northern lakes and the surrounding regional atmosphere. In section 2, we describe the models and the experiments. Section 3 evaluates the simulations of overlake meteorology, and section 4 compares the coupled and uncoupled model simulations, including seasonal timescale studies. Section 5 presents the conclusions.

2. Models and experiments

a. Atmospheric model

The atmosphere–lake coupled model consists of two components: the atmospheric model CRCM (version 3.4) and ocean model POM (1998 version). CRCM is based on the dynamical formulation of the Canadian Mesoscale Compressible Community (MC2) model and solves the fully elastic nonhydrostatic Euler equations using a semi-implicit semi-Lagrangian numerical scheme. The physical parameterization package of the second-generation Canadian Global Climate Model (GCMII), following McFarlane et al. (1992), is implemented to solve the subgrid-scale processes, and the Kain–Fritsch deep convection scheme replaces the GCMII moist adjustment scheme (Laprise et al. 2003).

The CRCM setup uses 29 vertical levels, 10 of which are below 850 hPa. Two sets of CRCM simulations are preformed, driven by the Canadian Meteorological Centre (CMC) 6-hourly analyses. A nine-point-wide sponge zone is used to interface the CRCM-simulated winds with the coarse-resolution outer-grid CMC driving fields, as indicated in Fig. 1a. The coarse-resolution model simulations are performed at a horizontal resolution of 51 km on a domain size of 100×90 grid points as shown in Fig. 1a. A 15-min time step is employed following MacKay et al. (2003). Clearly, the surface flux estimates from a 51-km resolution grid are too coarse to constitute representative forcing fields to drive the lake model, which has a 5-min (approximately 10 km) horizontal resolution. To improve the atmospheric model's resolution, the outputs of coarse-resolution model simulations are used to nest fine-resolution simulations, shown in Fig. 1b. This downscales the horizontal resolution to a 15-km resolution domain over Mackenzie River basin, with 135×160 grid points and a 15-min time step. The uncoupled version of CRCM assumes the surface corresponding to the lakes is land, with surface properties of adjacent land grid points and initial surface temperatures from CMC; after the initial time step, the GCMII physics determines the surface temperature over the lakes.

b. Lake implementation of POM

POM is implemented and customized for Great Bear Lake and Great Slave Lake. This is a three-dimensional, primitive equation model with complete thermohaline dynamics, using a sigma (σ) vertical coordinate and a free surface. A second-order turbulence closure scheme (Mellor and Yamada 1982) is used to represent the mixed layer dynamics. POM has been widely used to study major lakes and recently has been coupled to a regional climate model to study the impacts of Lake Victoria on the atmosphere (Song et al. 2004).

The bathymetry of Great Bear and Great Slave Lakes was digitalized from Canadian Hydrographic Service charts 6390, 6370, and 6341. To minimize pressure gradient errors, the bottom topography in the model was smoothed such that the difference in the depths of adjacent grid points divided by their mean is less than 0.4, following Mellor et al. (1994). Figure 2 shows the resulting interpolated bathymetry, after smoothing with the Laplacian filter and invoking the

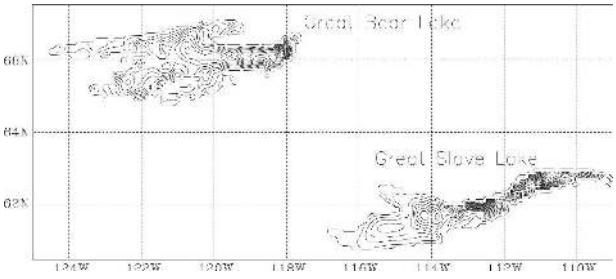

FIG. 2. POM domain and bathymetry showing 10-m depth intervals. Dotted lines are the boundaries of Great Bear Lake and Great Slave Lake.

slope adjustment. For both lakes, the eastern arms are much deeper than the western arms.

POM was implemented with a horizontal resolution of 5 min, on a latitude–longitude projection, giving a total of 1886 active lake grid points for the two lakes, as shown in Fig. 2. In the vertical coordinate, 13 σ layers are used (0.0, −0.048, −0.095, −0.143, −0.190, −0.238, −0.286, −0.333, −0.429, −0.571, −0.714, −0.857, −1.0), with the finest vertical resolution near the surface. To minimize pressure gradient errors (Mellor et al. 1994), we set the maximum depth to 210 m, neglecting several deeper subgrid areas. Time steps are 15 min for the internal baroclinic model and 15 s for the external mode. Closed lateral boundaries around each lake are used and there is no water exchange between rivers and lakes. Salinity is set to zero.

The initial water temperatures are prescribed, based on available observations (MacDonald et al. 2004). The water temperatures at the first four levels in Great Slave Lake gradually increase from 1°C at the first level to 4°C at the fourth level, while the water temperature elsewhere is set to 5°C. In Great Bear Lake, the water temperatures at the first three levels are 0.5°, 1°, and 2°C, respectively, and the temperatures elsewhere are set to 3°C. Great Slave Lake became ice free on 27 May 1998 and 10 June 1999, whereas Great Bear Lake became ice free on 29 June 1998 and 5 July 1999. The 1998 and 1999 simulations started on 1 June, and the model system is allowed a month to spin up, with output data analyzed only after 1 July. Although the lake model is initially slightly unstable, it reaches stability during the 1-month spinup. During this period, and until the lakes became ice free, no exchanges of surface fluxes are assumed to occur across the lake–atmosphere interface and the surface temperature is held near 0°C. This represents a simplified modeling of the impact of ice-melting processes, during which most of the received solar flux is used to melt the ice, the surface temperature is actually about 0°C, and the ice prevents the water from receiving fluxes.

c. Coupling technique

The coupled model system exchanges information between the atmosphere and lake at the air–water interface at every coupling time step. A typical simulation begins with the forward integration of the 15-km fine-resolution CRCM simulation for 1 time step (15 min) with fixed lake surface temperature. Wind stress and sensible and latent heat fluxes, radiative fluxes, and freshwater fluxes, as computed from CRCM, are transferred to POM. POM is then integrated forward for 15 min, which constitutes one time step of its baroclinic-mode time step, and produces a new surface temperature field that is then passed to CRCM, which in turn is integrated forward for another 15 min. Because of the different horizontal resolutions of the two models, data exchange between CRCM and POM is accomplished through interpolation from low resolution to high resolution and aggregation from high resolution to low resolution. Typically, bilinear interpolation is performed with the data from four grid points around a given output grid. However, some CRCM grid points near the lake shore are a mixture of lake and land points. For these grid points, the surface temperatures from the neighboring POM lake grid points are averaged to obtain the surface temperatures for a given CRCM grid point. The initial land surface temperature field, outside the lakes, is determined by data from the CMC analyses.

d. Experiment design

Under Canada's GEWEX program, a highly successful field campaign produced a novel dataset of atmospheric sounding and surface flux information in 1998 and 1999. These data provide insight into the atmospheric planetary boundary layer response to varying synoptic-scale regimes and the impacts of lake–atmosphere interactions. In this study, coupled and uncoupled simulations consist of CRCM, with or without the POM lake model. All the simulations start on 1 June and end on 31 October for both 1998 and 1999, allowing the model system to spin up during June in each year. Differing ice-free onset times in each year are accommodated. All the analyses started from 1 July, disregarding model outputs before that time. In the uncoupled experiment, the CRCM simulation does not include the feedbacks from lakes to the atmosphere. Comparisons between the coupled and uncoupled POM–CRCM simulations enable us to study the impacts of the lakes on water and energy cycles. Additional validation of simulations is achieved by comparisons with North American Regional Reanalysis (NARR) data, which have a 32-km horizontal resolution.

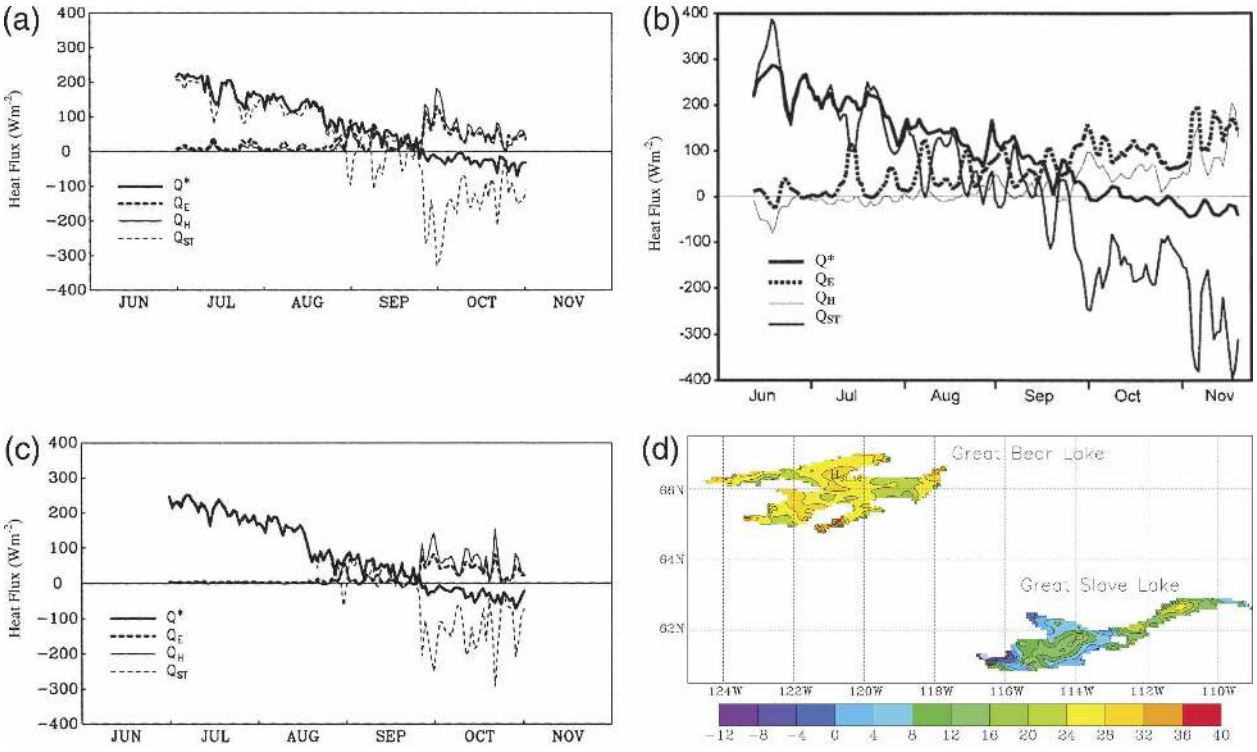

FIG. 3. (a) Energy balance over Great Slave Lake in 1999 simulated by CRCM–POM for time series of net radiation (Q*), latent heat flux (Q_E), sensible heat (Q_H), and total heat flux (Q_{ST}). Units are W m^{-2}. (b) Same as in (a) but for the observed 1999 Great Slave Lake time variations in Q*, Q_E, Q_H, and Q_{ST} from Rouse et al. (2003). (c) Same as in (a) but for the 1999 Great Bear Lake time variations in Q*, Q_E, Q_H, and Q_{ST} from the CRCM–POM coupled simulation. (d) The difference between the total heat flux (W m^{-2}) averaged over July–August 1998 minus the average for the same period in 1999.

3. Simulations of lake surface meteorology

a. Surface heat fluxes

The lake-averaged energy balances over Great Slave Lake simulated by the coupled CRCM–POM model are shown in Fig. 3a. Here, total heat flux (Q_{ST}) and net radiation flux (Q*) are positive when the lake gains heat, and latent heat flux (Q_E) and sensible heat (Q_H) are positive when the lake releases energy. In summer, Great Slave Lake receives heat flux from the atmosphere, whereas in the fall, this received summer heat is released back into the atmosphere. During the period from July to October, the total heat fluxes gradually decrease from about +200 W m^{-2} in early July to about −200 W m^{-2} in late October. The corresponding net radiation linearly decreases from about +200 W m^{-2} in early July to about −50 W m^{-2} in late October, which suggests that solar flux dominates the heat exchange between the atmosphere and the lake in the early summer. During midsummer, most of the received heat fluxes are net radiation fluxes; the latent and sensible heat fluxes are small. After September, the surface latent and sensible heat fluxes dominate the heat exchange between the lake and the atmosphere. Comparison between Figs. 3a,b suggests that the coupled model correctly produces the overall observed energy balance and time variations for Q*, Q_E, Q_H, and Q_{ST} for Great Slave Lake for July–October 1999. It is notable that CRCM underestimates the latent heat fluxes, especially in the summer, suggesting difficulties in simulating the latent heat fluxes in the GCMII physical package. Figure 3c shows corresponding time series for Great Bear Lake from the coupled model simulation, for which no observational data are available. Comparison between Figs. 3a,c suggests that the energy balances in Great Slave Lake and Great Bear Lake are similar. Smaller contributions of sensible and latent heat fluxes are more evident in Great Bear Lake in summer than in Great Slave Lake.

There was a transition from El Niño to La Niña during the period from June 1998 to September 1999; the associated air temperature across the Mackenzie basin is anomalously warmer in 1998 than in 1999 (Schertzer et al. 2003). Comparing these 2 yr gives an indication of the lake model's ability to respond to interannual variations of surface heat fluxes. To give an area illustration

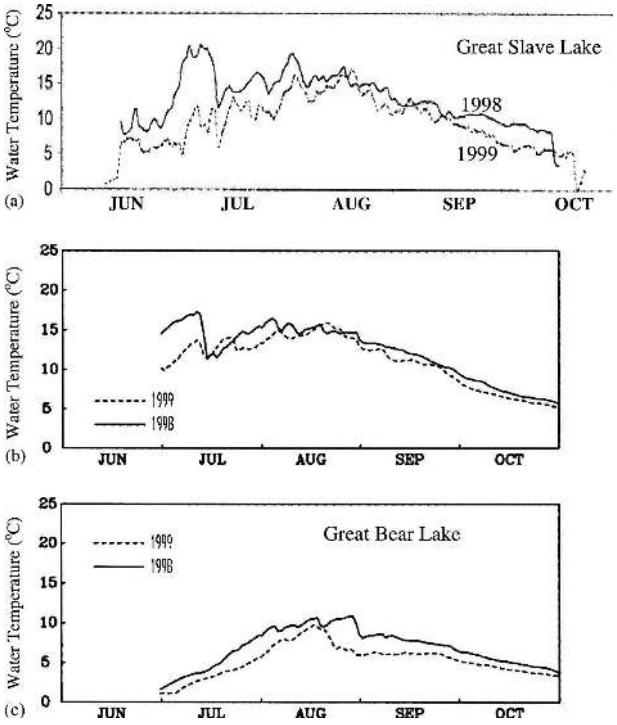

FIG. 4. Surface temperature (°C) averaged over Great Slave Lake in 1998 and 1999, showing (a) observations (from Schertzer et al. 2003) for 1998 (solid) and 1999 (dashed) and (b) simulations for 1998 (solid) and 1999 (dashed). (c) Same as in (b), but simulated surface temperature (°C) over Great Bear Lake in 1998 (solid) and 1999 (dashed), lakewide averaged over the entire lake.

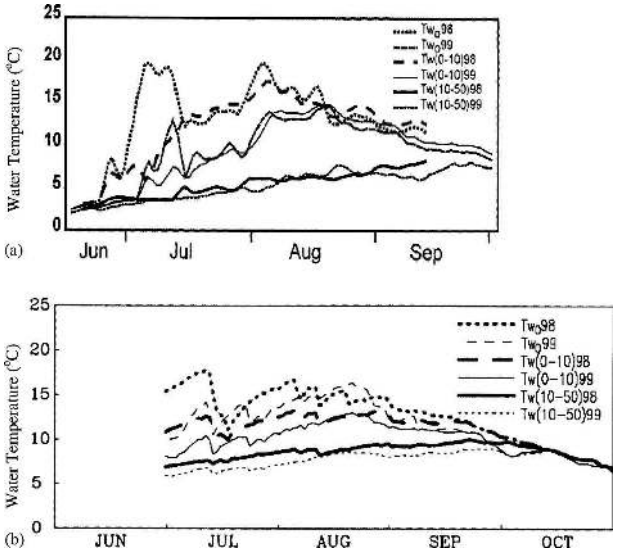

FIG. 5. Same as in Figs. 4a,b, but showing water temperature (°C) over Great Slave Lake: at the surface Tw_o, averaged over the 1–10-m depth, Tw(0–10), and averaged over the 10–50-m depths, Tw(10–50), for (a) observations (from Rouse et al. 2003) and (b) simulations.

of this difference, Fig. 3d shows the total lake heat flux for 1998, averaged over the July–August period, *minus* that of 1999. Although both lakes received more heat flux during the summer of 1998 than in 1999, the difference is particularly evident for Great Bear Lake, where most of the lake received an average of 24 W m^{-2} more heat flux in July–August of 1998 than in the same period of 1999. In any case, areas of either lake that achieved early ice-free status show the strongest differences in heat fluxes, reflecting the different large-scale atmospheric circulation patterns of these 2 yr.

b. Water temperature

Great Slave Lake's surface water temperatures, corresponding to its surface fluxes, are shown in Figs. 4a,b, averaged over the entire lake for 1998 and 1999. In early summer, the surface water temperature gradually increases, and the lake becomes warmest in early August. Thereafter, particularly after late August, the water temperature steadily decreases. Comparison with observations suggests that the coupled model gives a good simulation of the overall magnitude and variation of surface water temperature. Both the simulation and observations show that the lake reaches about 15°C maximum temperature in early August, and this temperature persists until late August. However, coupled model simulations of Great Slave Lake do not show the sharp decrease in temperature in October that is seen in the observations. This bias is related to an inadequate representation of ice processes in the lake model and the warm bias at 10–50 m seen in Fig. 5.

Great Slave Lake became ice free a couple of weeks earlier in 1998 than in 1999, which is consistent with the 1997/98 El Niño atmospheric circulation anomaly. This early thaw in 1998 had significant influence on surface water temperature in early July, as shown in Figs. 4a,b. Both the observations and the coupled model simulation suggest that the surface water temperatures were about 5°C warmer in 1998 than in 1999. However, the simulation tends to underestimate the surface temperature peak in early July 1998. At that time, surface water temperatures were observed above 20°C in Great Slave Lake, whereas the simulated peak was about 17°C. After mid-July, the observed impact of the early ice-free state on the surface water temperature in Great Slave Lake was much weaker (Fig. 4a). Similar results can be found in the simulation of Great Bear Lake, as shown in Fig. 4c, enhanced early warming and later cooling in 1998 compared to 1999. However, the latter reaches its maximum temperature a couple of weeks later than Great Slave Lake.

Large interannual temperature variations were ob-

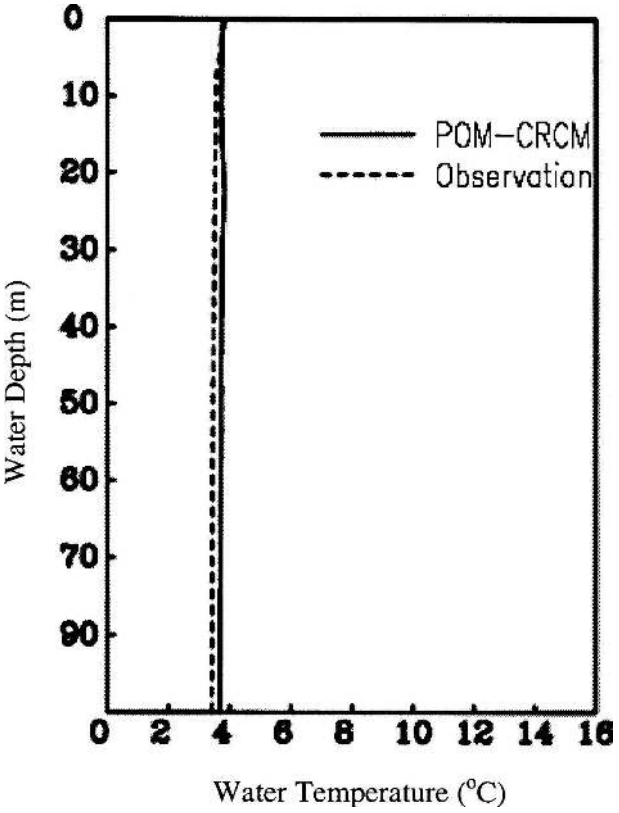

FIG. 6. Vertical profiles of water temperature (°C) at 10 km west of Port Radium, comparing averaged observations for August 1964 and 1965 (dashed) and coupled model simulation for August 1999 (solid). The 1964–65 data are available on the International Lake Environment Committee Foundation (ILEC) Web site at http://www.ilec.or.jp/database/nam/nam-30.html.

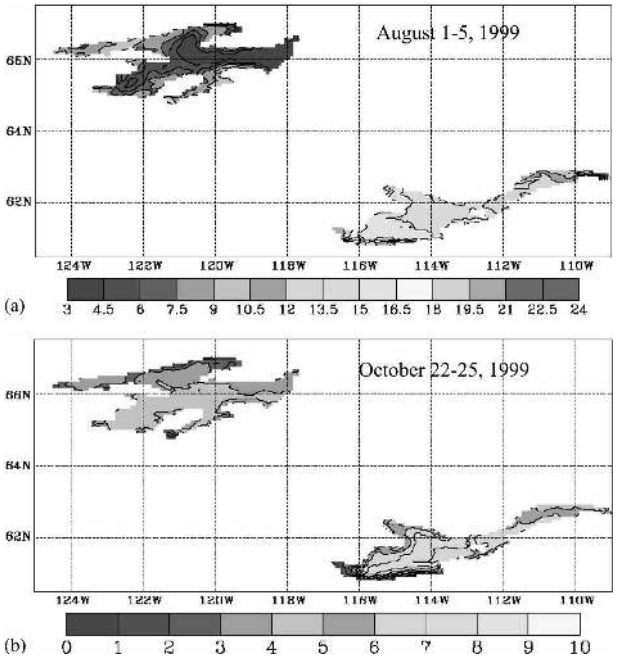

FIG. 7. Surface temperature (°C) for the two lakes (a) on 1–5 Aug 1999 and (b) on 22–26 Oct 1999.

served in the upper water column of Great Slave Lake, particularly in the top 10 m, which is consistent with surface water observations. This is shown by field observations from Inner Whaleback Islands, located at 61.92°N, 113.73.73°W, as presented by Rouse et al. (2003), as well as by our coupled simulations in Figs. 5a,b. However, at greater depths, such as 10–50 m, Rouse et al. (2003) suggest that water temperatures in 1998 show no evident difference compared to those of 1999. This is also consistent with our coupled model simulations in Fig. 5b. In the case of either observations or simulations, the depth-averaged (10–50 m) water temperatures increase slightly as the season progresses, until the end of September, and begin to decrease thereafter. It is notable that the simulations overestimate the temperatures at 10–50 m in Great Slave Lake, compared with the observations, with a model bias of about 4°C.

Figure 6 shows the coupled model simulation of the vertical profile of water temperature in McTavish Arm at 10 km west of Port Radium (66.05°N, 117.55°W) for August 1999 and the available averaged observations. For the water temperature, only the data collected from 1964 and 1965 have been published (Johnson 1994; http://www.ilec.or.jp/database/nam/nam-30.html). Both observations and the coupled model simulation suggest that Great Bear Lake is well mixed, because the temperatures are similar from top to bottom at about 3.5°C. Compared with observations, the modeled water temperature in 1999 is slightly warmer than the observations during 1964–65. Comparing Great Slave Lake with Great Bear Lake, the former was strongly stratified, with the surface water temperature about 10°C higher than at 50 m (Fig. 5b). This discrepancy in stratification reflects the difference in the ice break-up dates between the two lakes. Through both in situ and satellite observations, it is well known that ice breakup on Great Slave Lake typically precedes that on Great Bear Lake by about one month. Because of a relatively late ice breakup in Great Bear Lake in 1999, Great Slave Lake gained more solar flux to warm the upper water levels than Great Bear Lake. Correspondingly, in early summer, the stratification in Great Slave Lake is more stable (warmer in the upper layer) and this lake becomes less mixed than is the case for Great Bear Lake. Because the upper-layer water is very cold in the Great Bear Lake, it is well mixed.

Finally, we consider the distribution of modeled surface lake temperatures over the areas of the two lakes (Fig. 7). During the open-water warming phase, from

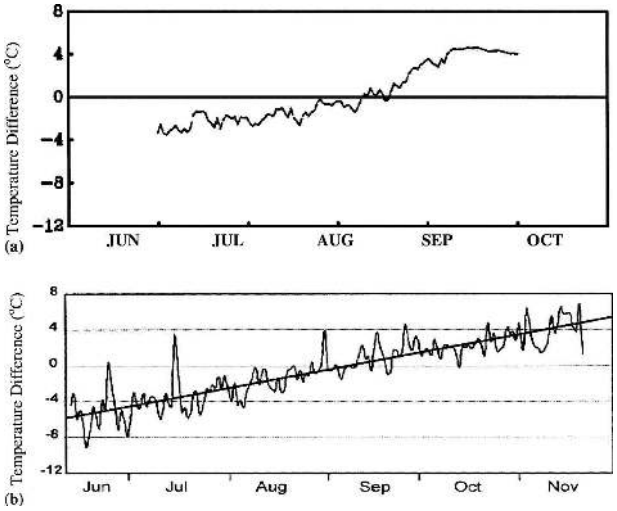

FIG. 8. Temperature (°C) difference times series between central Great Slave Lake at Inner Whaleback Islands (61.92°N, 113.73.73°W) and Yellowknife Airport (62.45°N, 114.40°W), (a) coupled model simulation for 1999 and (b) averaged difference for 1997–99 (from Rouse et al. 2003).

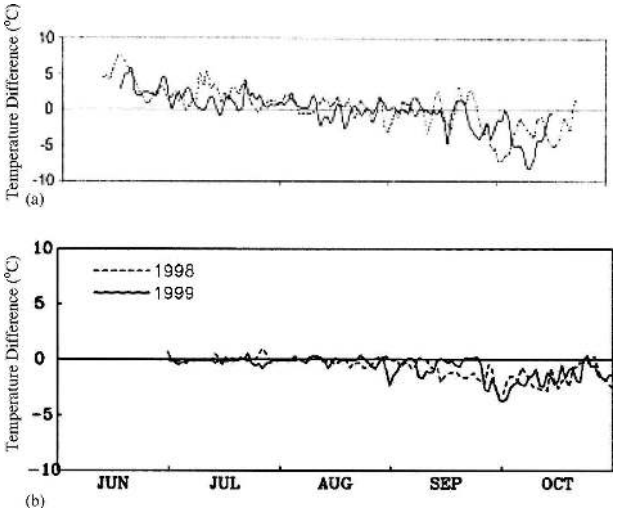

FIG. 9. Lake-averaged time series of air minus water temperatures (°C) over Great Slave Lake for (a) observations (from Schertzer et al. 2003) in 1998 (dashed) and 1999 (solid) calculated as averages along seven observing stations transecting the center of the lake and (b) coupled simulation in 1998 (dashed) and 1999 (solid), calculated as lakewide averages for all water grid points.

late June until late August, the lake surface waters tend to be warmest near the western and central shorelines and coldest in the deepest waters in both lakes and in the easternmost regions, reflecting the bathymetry. This is shown in Fig. 7a for 1–5 August 1999. Conversely, in the associated cooling phase, from late August until late October, the surface water is warmest in the central portion of the lake and tends to be coldest near the western shore in Great Slave Lake. In Great Bear Lake, the surface temperature is almost uniform, with the northern and western portions of the lake arms tending to be slightly colder than the central portions of the lake. This is shown in Fig. 7b for 22–26 October 1999.

c. Surface air temperature

The differences in surface air temperatures between Inner Whaleback Islands located at 61.92°N, 113.73.73°W in Great Slave Lake and nearby Yellowknife Airport (62.45°N, 114.40°W) are shown in Figs. 8a,b. Both the observed data and the corresponding coupled model simulation show that the differences in temperature increase from −4°C in July to +4°C in October. This suggests that the coupled model is capable of representing the land–lake contrast in Great Slave Lake. Figure 9 shows the difference between the surface air temperature and the surface water temperature, averaged over Great Slave Lake. The coupled model is able to simulate the negative air–lake temperature difference tendency in October, which is consistent with the fact that the lake releases latent and sensible heat fluxes into the atmosphere, as shown in Fig. 3a. However, the simulated October negative temperature difference is weaker than the observed data difference; in summer, the model simulation shows negligible temperature difference (surface air minus surface water), whereas a small positive difference occurs in the observed data. Hence the differences are systematically underestimated; in part, this may be the result

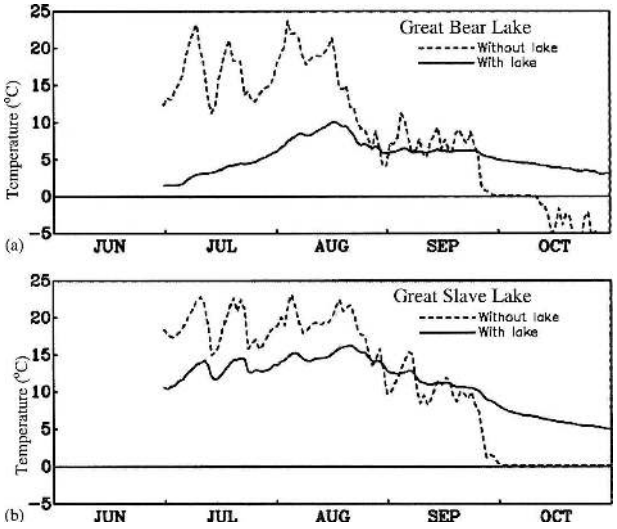

FIG. 10. Lakewide-averaged surface temperature (°C) in 1999 for simulations with (solid) and without (dashed) the lake for (a) Great Bear Lake and (b) Great Slave Lake.

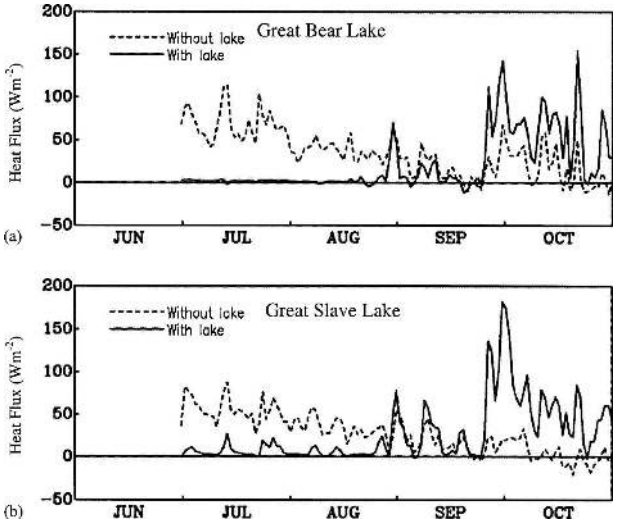

FIG. 11. Same as in Fig. 10 but showing lakewide-averaged surface sensible heat flux (W m^{-2}) in 1999 for simulations with (solid) and without (dashed) the lake for (a) Great Bear Lake and (b) Great Slave Lake.

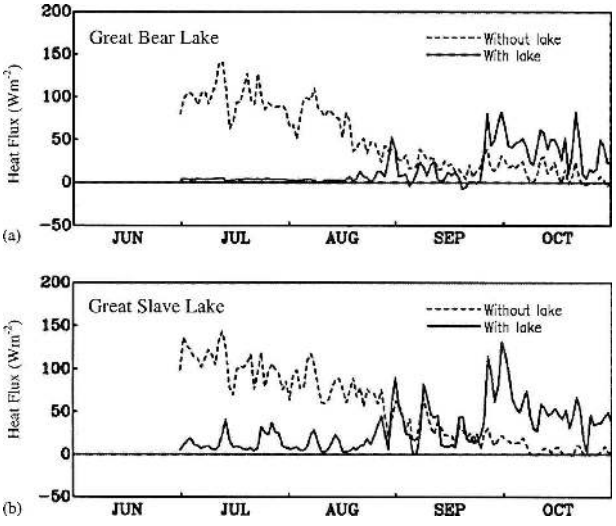

FIG. 12. Same as in Fig. 11 but showing lakewide-averaged latent heat transport from lake surface (W m^{-2}) in 1999 for simulations with (solid) and without (dashed) the lake for (a) Great Bear Lake and (b) Great Slave Lake.

of the relatively crude algorithm used in CRCM to estimate the screen-level temperatures from the lowest model prognostic level. Another factor in the difference between the observed and modeled temperatures is the fact that the observed plot is the average from only seven stations and the modeled plot is constructed from a total surface average.

d. Lake impacts on the overlake variables

The simulated (with and without lakes) lake-averaged surface temperatures in 1999 are shown in Fig. 10. In the uncoupled simulation (without lakes), the surface temperature over Great Bear Lake is about 10°C higher than in the coupled model simulation in July–August and about 10°C lower in October. There are no significant differences from the end of August to the end of September (Fig. 10a). A similar pattern can be seen in Great Slave Lake (Fig. 10b). Comparisons between Figs. 10a,b show that Great Bear Lake has a notably stronger impact on the simulations of lake surface temperature than Great Slave Lake. As shown in Figs. 3a–c, the lakes receive significant net radiation from the air in July, but in September, there are no significant heat fluxes into the lakes. Thus, there is a warm anomaly in July but not in September, as presented in Figs. 10a,b.

Corresponding to the temperature time series patterns, uncoupled simulations (without the lake) result in overestimates in the surface sensible and latent heat fluxes in summer (July–August) and underestimates in these surface heat fluxes in October. The associated summer overestimate in the surface sensible heat fluxes is more than 50 W m^{-2} and the October underestimate by more than 50 W m^{-2} (Figs. 11a,b). Furthermore, uncoupled simulations result in a summer overestimate in latent heat transport from the lake surface (as estimated from surface evaporation) by about 100 W m^{-2} and an October underestimate by about 50 W m^{-2} (Figs. 12a,b). The impacts of northern lakes on regional surface heat exchanges between the lake and the atmosphere are therefore significant.

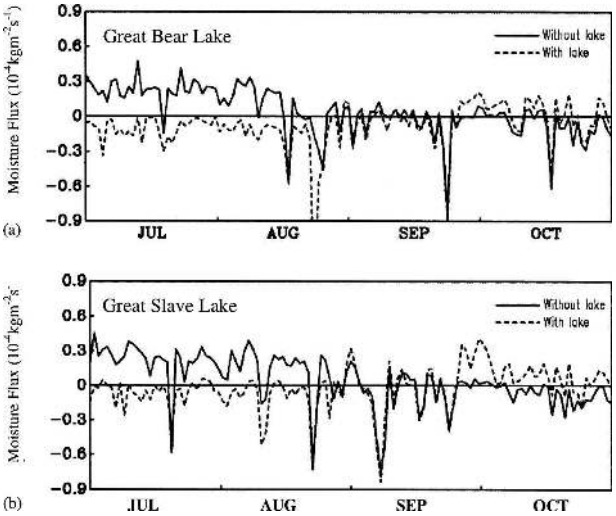

FIG. 13. Same as in Fig. 11 but showing lakewide-averaged moisture flux in 1999 for simulations without (solid) and with (dashed) the lake for (a) Great Bear Lake and (b) Great Slave Lake. Units are 10^{-4} kg m^{-2} s^{-1}.

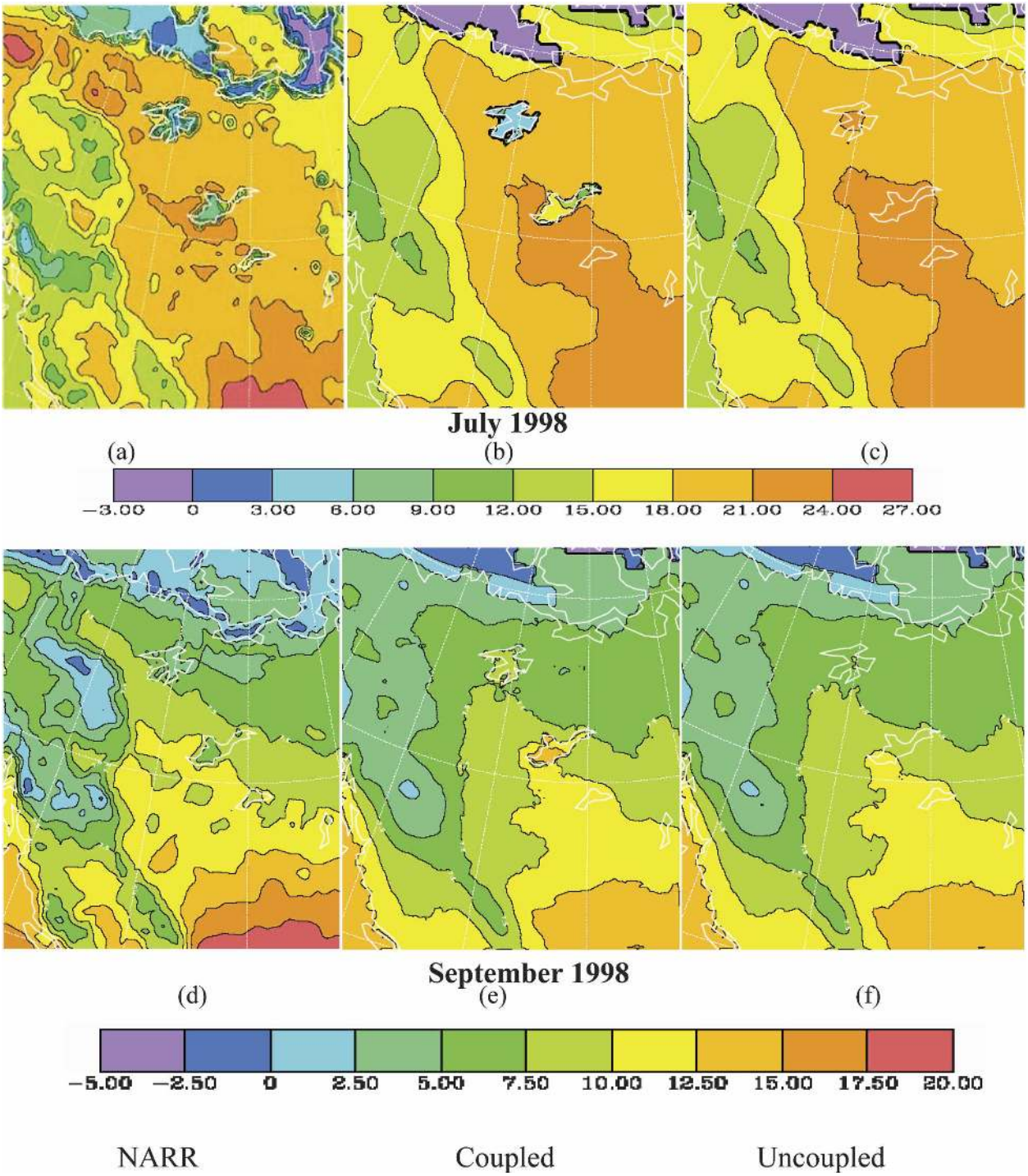

FIG. 14. Monthly averaged surface temperature (°C) in July 1998: (a) NARR, (b) coupled POM–CRCM simulation, and (c) uncoupled CRCM simulation and also for September in 1998: (d) NARR, (e) coupled POM–CRCM, and (f) uncoupled CRCM.

The associated impacts of northern lakes on surface moisture exchanges are shown in Figs. 13a,b. As with the surface heat exchange simulations, these simulations suggest that the northern lakes have significant impacts on the surface moisture exchanges over the lakes. Compared to uncoupled simulations, the coupled simulations suggest that the lakes introduce large seasonal thermal lags due to their large heat capacities,

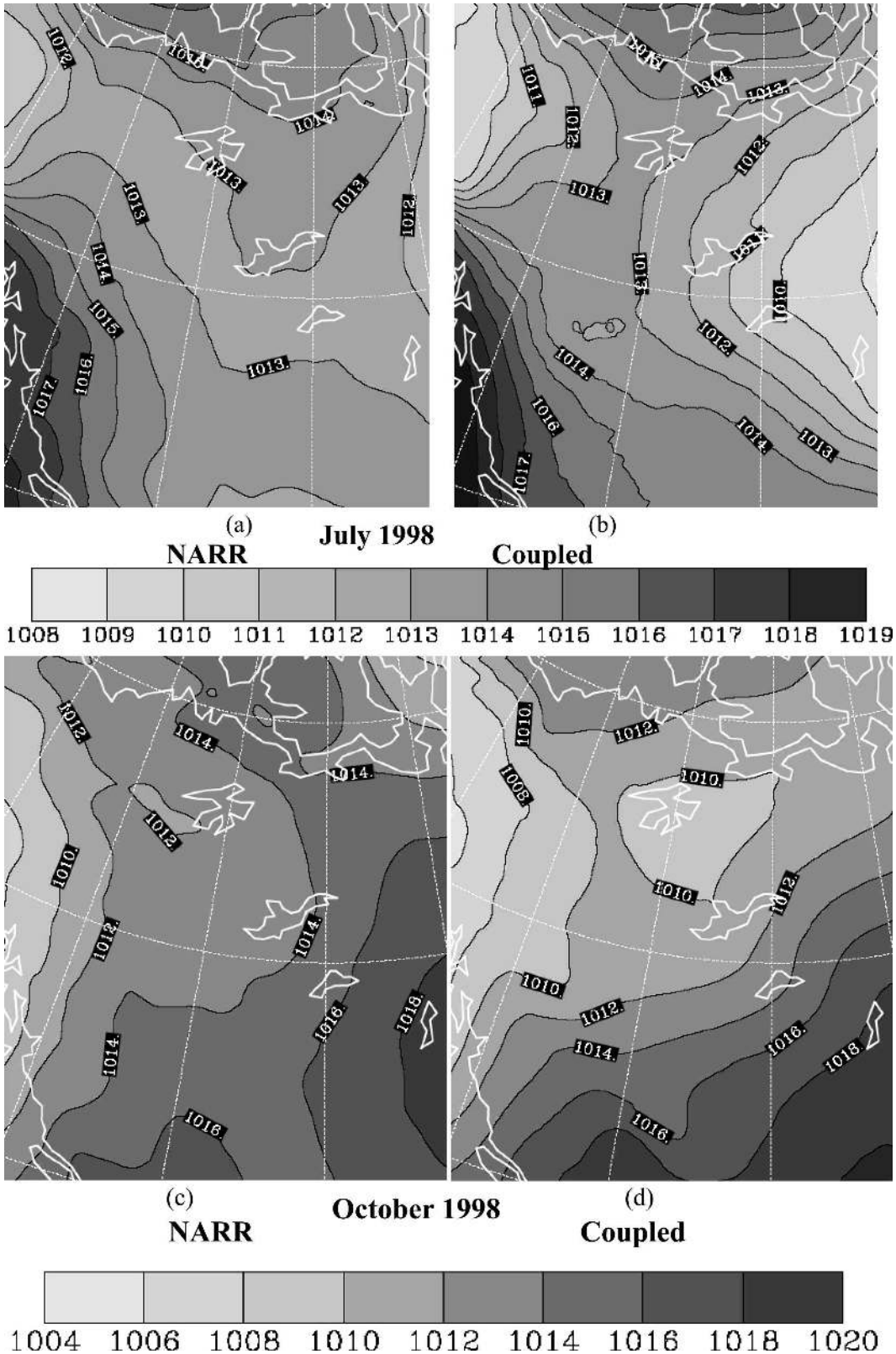

FIG. 15. Averaged SLP in July 1998 for (a) NARR and (b) coupled POM–CRCM simulation. Units are hPa. SLP (hPa) in October 1998 for (c) NARR and (d) coupled simulation.

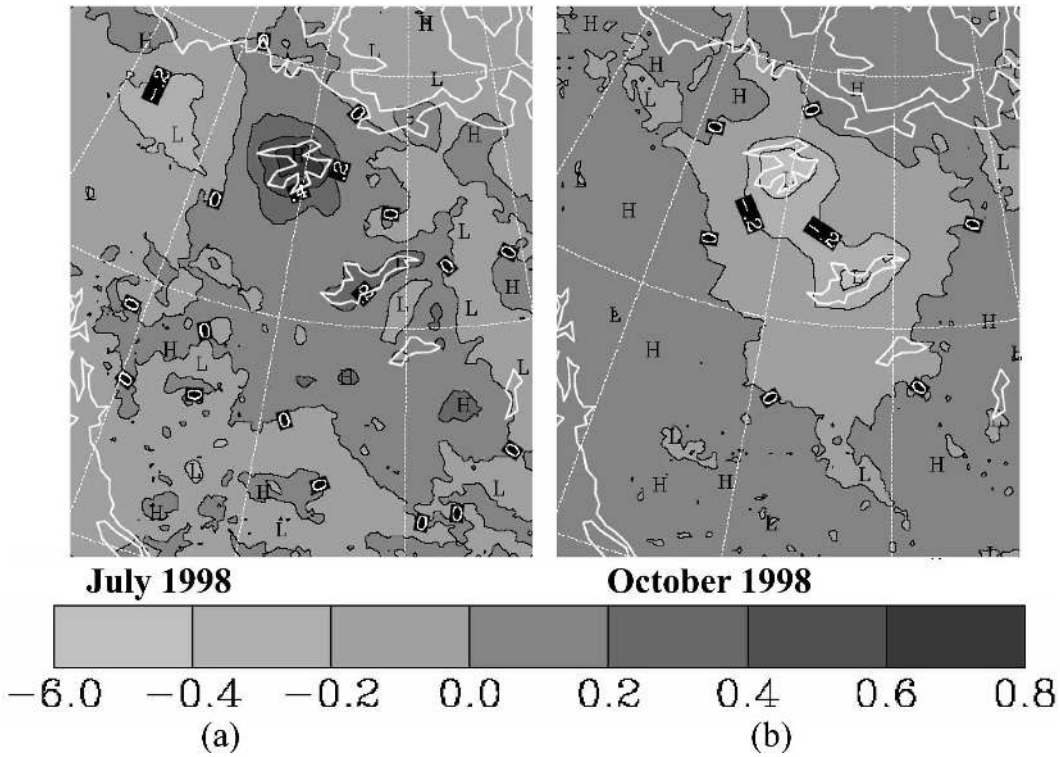

FIG. 16. SLP (hPa) differences between coupled simulation minus the uncoupled simulation for (a) July and (b) October 1998. Local maxima in SLP differences are denoted by H, and local minima are denoted by L.

resulting in reductions in moisture fluxes by about 3×10^{-5} kg m^{-2} s^{-1} in July–August and enhanced moisture fluxes in the fall.

4. Lake–atmosphere impacts on regional climate and weather

a. Surface temperature

Monthly averaged surface temperatures for July 1998, comparing NARR data to coupled and uncoupled model simulations, are shown in Figs. 14a–c. Relative to the NARR data and the uncoupled model, the coupled model can simulate the surface temperature in the Mackenzie basin relatively well; Fig. 14b shows a strong temperature ridge in the Mackenzie basin with temperatures above 17°C in most of the region and surface temperatures in Great Bear Lake and Great Slave Lake that are much lower than the surrounding land surface temperatures. Both NARR and the coupled simulation suggest about 5°C surface temperature in Great Bear Lake. In Great Slave Lake, the surface temperature in the coupled model simulation is around 15°C, which is significantly higher than the NARR surface temperature. However, observations (Fig. 4a) suggest that the NARR data underestimate the surface temperature in Great Slave Lake in July 1998 by several degrees (Schertzer et al. 2003). Comparing uncoupled and coupled simulations (Figs. 14b,c) suggests that the latter can improve the surface temperature estimates around the lake regions and also clearly shows the impacts of the lakes.

Similar results are also given in Figs. 14d,f for September 1998. The coupled model simulation suggests that the surface temperatures are higher over both lakes than over the surrounding land, and thus the lakes act as heat sources (Fig. 14e), which is consistent with the field observations (Fig. 8b). Meanwhile, the NARR data suggests that the lakes are colder than the surrounding land in September, which is inconsistent with station observations (Figs. 4a, 8b, and 9a) and underestimates the lake surface temperature fields in both lakes.

b. Sea level pressure

Figures 15a–d show the monthly averaged sea level pressure (SLP) in July and October for NARR analysis fields and the coupled model simulation. This shows that, relative to the NARR data, the coupled model can simulate the SLP field well. In particular, the overall pressure ridge over the northern part of the

high-resolution CRCM domain in July is well represented. In October, both NARR and the coupled simulation show a low pressure system extending toward the northeast, from west of the Mackenzie River basin. The corresponding SLP differences between coupled and uncoupled model simulations are shown in Fig. 16. On the monthly time scale, the impacts of both lakes on SLP are small, less than 1 hPa; in July the SLP difference near the lakes is slightly positive, but in October it is slightly negative.

c. Screen-level specific humidity

As discussed above, Great Slave and Great Bear Lakes have significant impacts on the local surface temperature. Typically, the surface temperatures over the lakes are as much as 4°C lower than the surrounding land surface temperatures in July (Fig. 8). This has significant impact on the overlake surface moisture. Figures 17a,b show the differences of screen-level specific humidity between the coupled and uncoupled simulations. The differences are notable near the lakes; they are clearly negative in July and positive in October. In July (Fig. 17a), the lakes are able to modify the regional distribution of surface specific humidity within the scale of the Mackenzie River basin. Over the lake regions, the specific humidity is much lower than the surrounding regions due to their cold temperatures. In October (Fig. 17b), however, because the surface temperatures over the lakes are much warmer than over the surrounding land (Fig. 8), the specific humidity over the lakes is therefore also much higher than that over the surrounding land (Fig. 17b). This shows the importance of the lakes in simulations of surface moisture processes.

d. Lake impacts on snow

Surface moisture processes are related to the snow field that is expected to accumulate around the lakes, beginning in the autumn. Accumulation of snow on the ground impacts the local water cycle, acting as short-term surface water storage. It also influences the local surface energy cycle through its effect on the albedo, and thus it is important to understand how the lakes can influence snow.

The monthly averaged distributions of snow for October 1998, simulated by CRCM with and without lakes, are given in Figs. 18a,b. In October 1998, although the snow accumulation around Great Slave Lake is slight, the simulations suggest that the snow around Great Bear Lake is significant, particularly to the north and west of the lake, and also in isolated mountain areas to the southwest of the lakes. However

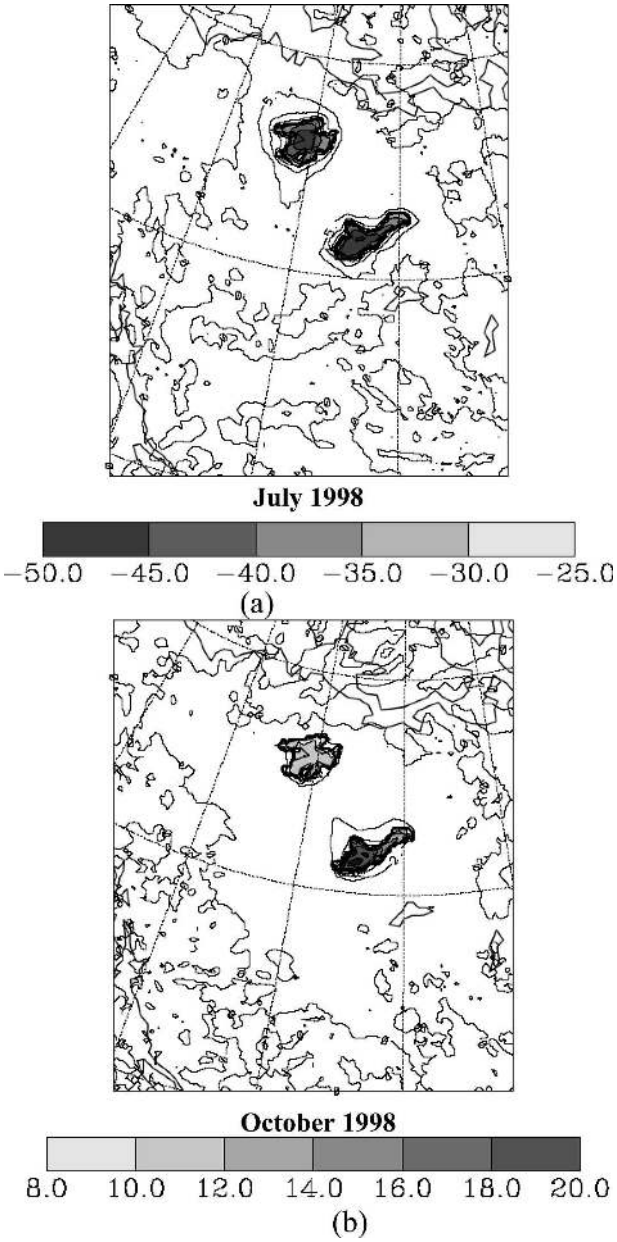

FIG. 17. Differences in screen specific humidity between coupled and uncoupled model simulations for (a) July and (b) October 1998; units: 10×10^4 kg kg^{-1}.

the NARR analyses (Fig. 18c) suggest that CRCM overestimates snow accumulation to the north of the lake but underestimates snow accumulation to the west.

Figures 19a,b show the differences (coupled minus uncoupled) for monthly and last-half monthly October averages. These results suggest that Great Bear Lake, and to a lesser extent Great Slave Lake, reduces the accumulation of snow on the ground around the lake area. In the area around Smith Arm at the western end of Great Bear Lake, there is a clear accumulation of

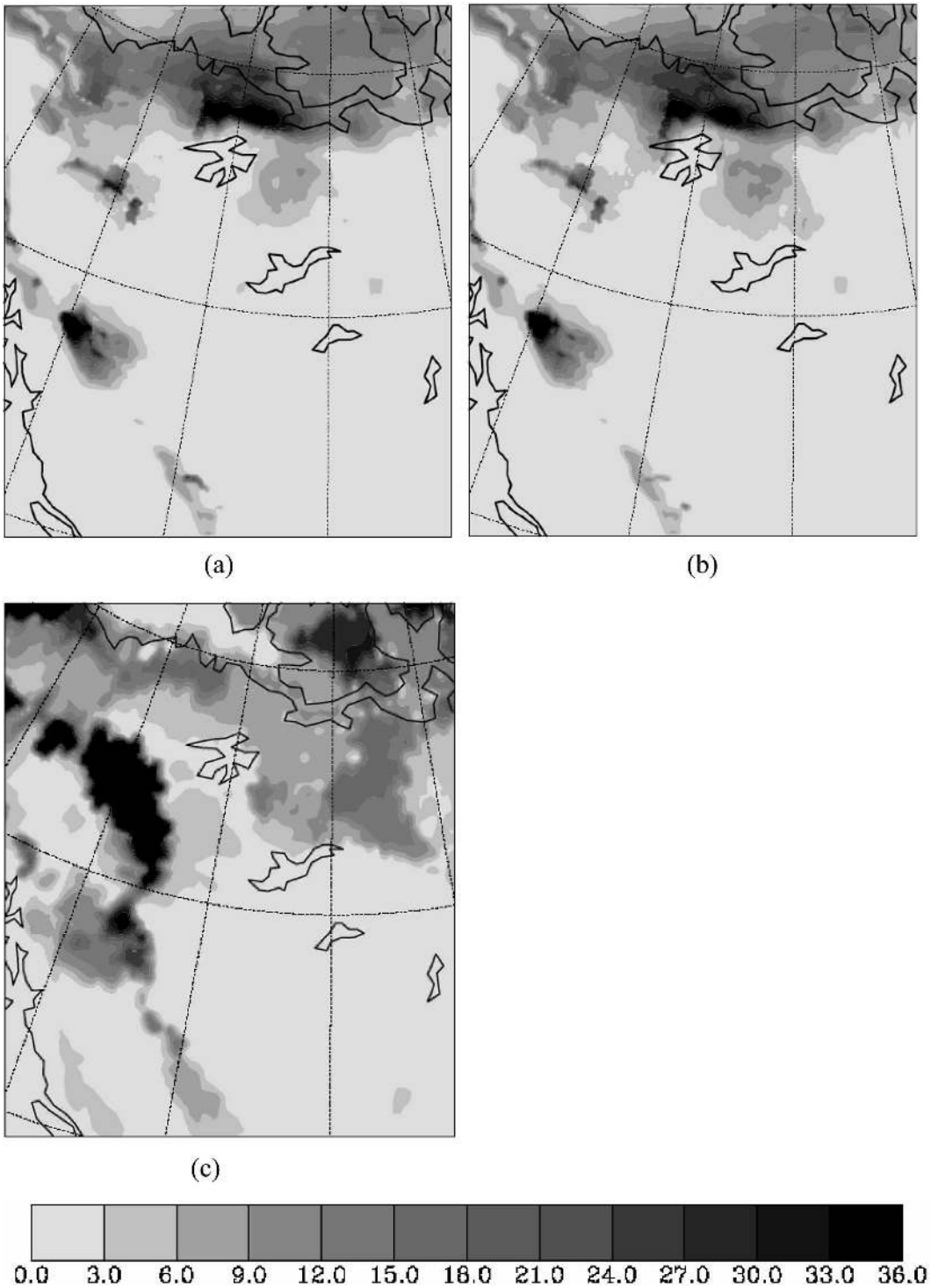

FIG. 18. Averaged snow accumulation on the surface (kg m^{-2}) for the second half of October 1998: (a) coupled POM–CRCM, (b) uncoupled CRCM, and (c) NARR.

snow in the uncoupled simulation, which is absent in the coupled simulation. To the west and northwest of Great Bear Lake, the snow in the coupled simulation is notably less than that suggested by the uncoupled simulation; however, increased snow is evident to the north of the lake indicating increased moisture. As presented in Fig. 3, Great Bear Lake is a heat source in October, as is Great Slave Lake to a lesser extent, through the

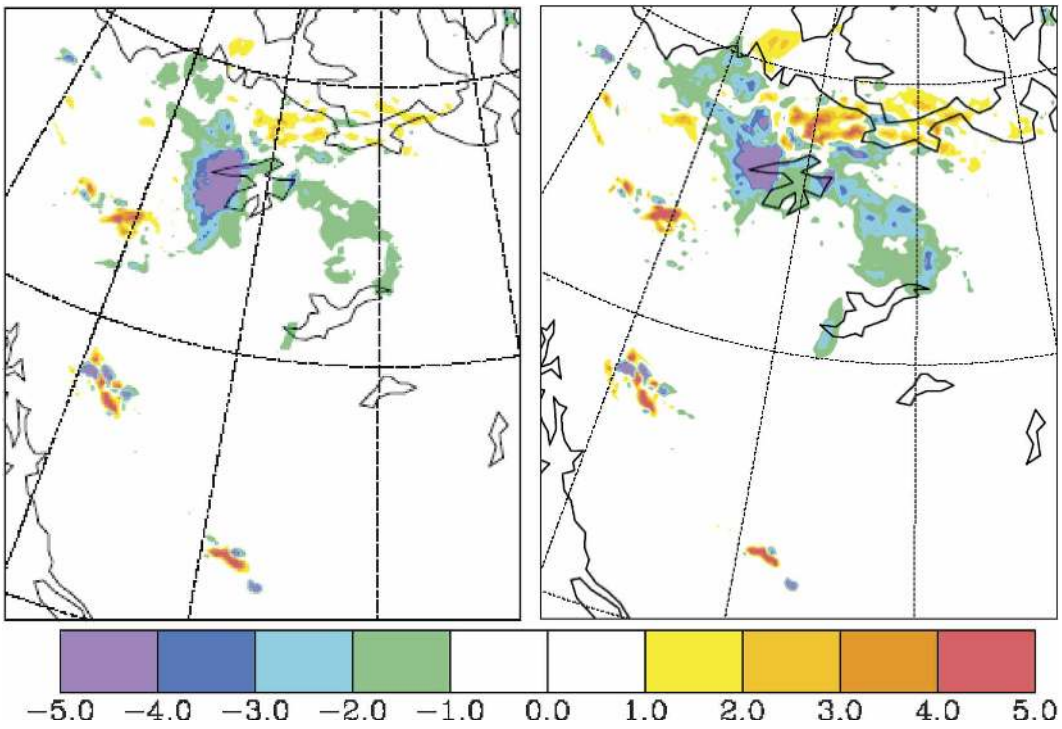

FIG. 19. Same as in Figs. 18a,b but showing (a) difference in monthly averages for average snow accumulation on the surface (kg m^{-2}) for October 1998 (coupled minus uncoupled simulations) and (b) difference in averages for the last half of October 1998.

release of latent and sensible heat fluxes. Thus the accumulation of snow in the local surrounding land area is reduced.

5. Conclusions

The Princeton Ocean Model (POM) was implemented to simulate Great Bear Lake and Great Slave Lake and coupled to the Canadian Regional Climate Model (CRCM) to simulate the regional atmosphere–lake interactions. Comparisons between our simulations and the observations of Schertzer et al. (2003) and Rouse et al. (2003) suggest that the coupled lake–atmospheric model can provide good representations of the overlake heat fluxes and water temperatures. In summer, the surface latent and sensible heat fluxes are small, and net downward radiation fluxes are dominant, warming these lakes, and thus the lakes act as energy sinks. In the autumn, the net downward radiation fluxes are small, and the surface sensible heat and latent heat fluxes dominate the energy exchanges between the lakes and the atmosphere.

During the (ice free) warming phase, the northern lakes tend to be warmest near the shore areas and coldest in the deepest lake areas. During the cooling phase, the cooling process in Great Bear Lake is different from that of Great Slave Lake. In the fall, Great Slave Lake is coldest near the shore areas and warmest in deep water. In Great Bear Lake, the eastern areas of the lake are slightly colder than the western areas of the lake, but the water temperatures are more uniform than in Great Slave Lake. The coupled model was successful in simulating the vertical temperature profiles in both lakes, as well as the lakes' responses to the differing surface heat fluxes in the El Niño year 1998, compared to 1999.

Due to their large heat capacities, the northern lakes have significant impacts on surface heat and moisture fluxes. In summer, coupled simulations and observed surface temperatures over the lakes are colder than uncoupled simulations; the lakes tend to reduce the fluxes of surface latent and sensible heat. However, in the fall, surface temperatures over the lakes are warmer than the uncoupled simulations; the lakes tend to increase the latent and sensible heat fluxes. During July–August, the net radiation used to warm these lakes is an average of 126 W m^{-2} in Great Slave Lake and 155 W m^{-2} in Great Bear Lake. This energy is released during the fall and winter. In October, the released energy through sensible and latent heat fluxes is about 135 W m^{-2} in

Great Slave Lake and 125 W m^{-2} in Great Bear Lake. Thus, northern lakes have important impacts on the local water and energy cycles.

Comparison with NARR analysis fields suggests that the coupled simulations give good representations of the local surface temperature and sea level pressure. However, the simulated interannual variation of surface temperatures over the lake regions is slightly weak, comparing model results to observed 1998 and 1999 data. On the monthly time scale, the impacts of both lakes on SLP are also weak, although both lakes can notably impact the surface moisture processes over lake regions. In the autumn, the release of latent and sensible heat fluxes acts as a heat source, reducing the snow accumulation in the surface areas around the lakes. This is particularly evident in simulations around Great Bear Lake.

It is important to note that there are similarities between the impacts of northern lakes and those of lower-latitude lakes (Lofgren 1997). For example, both the northern lakes and the Great Lakes reduce the surface temperature and evaporation during summer and increase the surface temperature and evaporation during the fall and winter. They act as energy sinks in the early summer and energy sources in the fall. The warming of the northern lakes during the spring and early summer tends to occur in the shallower areas first, leaving a pool of cold water in the deeper areas, which is similar to studies of Lake Michigan (Beletsky and Schwab 2001). In the fall, the cooling starts from the shallower areas, particularly in the Great Slave Lake. As with the Great Lakes, our coupled model simulations of northern lakes show obvious phase shifts in the seasonal variations of latent and sensible heat fluxes, compared to uncoupled simulations. However, there are also differences between the Great Lakes and the northern lakes; Great Bear Lake is well mixed due to its higher latitude, which is not the case for lower-latitude lakes.

Acknowledgments. This work was funded by Canadian Foundation on Climate and Atmospheric Studies (CFCAS) and by Canada Panel of Energy Research and Development funding for "Extreme Storms and Waves."

REFERENCES

Bates, G. T., F. Giorgi, and S. W. Hostetler, 1993: Toward the simulation of the effects of the Great Lakes on regional climate. *Mon. Wea. Rev.,* **121,** 1373–1387.

Beletsky, D., and D. J. Schwab, 2001: Modeling circulation and thermal structure in Lake Michigan: Annual cycle and interannual variability. *J. Geophys. Res.,* **106,** 19 745–19 771.

Blanken, P. D., W. R. Rouse, and W. M. Schertzer, 2003: Enhancement of evaporation from a large northern lake by the entrainment of warm, dry air. *J. Hydrometeor.,* **4,** 680–693.

Bonan, G. B., 1995: Sensitivity of a GCM simulation to inclusion of inland water surfaces. *J. Climate,* **8,** 2691–2704.

Caya, D., and R. Laprise, 1999: A semi-implicit semi-Lagrangian regional climate model: The Canadian RCM. *Mon. Wea. Rev.,* **127,** 341–362.

Hostetler, S. W., G. T. Bates, and F. Giorgi, 1993: Interactive coupling of a lake thermal model with a regional climate model. *J. Geophys. Res.,* **98,** 5045–5057.

Johnson, L., 1994: Great Bear Lake. *The Book of Canadian Lakes,* R. J. Allen et al., Eds., Canadian Association on Water Quality, 549–559.

Laprise, R., D. Caya, A. Frigon, and D. Paquin, 2003: Current and perturbed climate as simulated by the second-generation Canadian Regional Climate Model (CRCM-II) over northwestern North America. *Climate Dyn.,* **21,** 405–421.

Lofgren, B. M., 1997: Simulated effects of idealized Laurentian Great Lakes on regional and large-scale climate. *J. Climate,* **10,** 2847–2858.

MacDonald, D. D., D. A. Levy, A. Czarnecki, G. Low, and N. Richea, 2004: State of the aquatic knowledge of Great Bear Watershed. Prepared for Water Resources Division Indian and Northern Affairs Canada, MacDonald Environmental Sciences Ltd., 144 pp.

MacKay, M. D., F. Seglenieks, D. Verseghy, E. D. Soulis, K. R. Snelgrove, A. Walker, and K. Szeto, 2003: Modeling Mackenzie basin surface water balance during CAGES with the Canadian Regional Climate Model. *J. Hydrometeor.,* **4,** 748–767.

McFarlane, N. A., G. J. Boer, J.-P. Blanchet, and M. Lazare, 1992: The Canadian Climate Centre second-generation general circulation model and its equilibrium climate. *J. Climate,* **5,** 1013–1044.

Mellor, G. L., 1998: User's guide for a three-dimensional primitive equation numerical ocean model. Program in Atmospheric and Oceanic Sciences, Princeton University, 35 pp.

——, and T. Yamada, 1982: Development of a turbulent closure model for geophysical fluid problems. *Rev. Geophys.,* **20,** 851–875.

——, T. Ezer, and L. Y. Oey, 1994: The pressure gradient conundrum of sigma coordinate ocean models. *J. Atmos. Oceanic Technol.,* **11,** 1126–1134.

Rouse, W. R., and Coauthors, 2003: Energy and water cycles in a high-latitude, north-flowing river system: Summary of results from the Mackenzie GEWEX Study—Phase I. *Bull. Amer. Meteor. Soc.,* **84,** 73–87.

Schertzer, W. M., W. R. Rouse, P. D. Blanken, and A. E. Walker, 2003: Over-lake meteorology and estimated bulk heat exchange of Great Slave Lake in 1998 and 1999. *J. Hydrometeor.,* **4,** 649–659.

Small, E. E., and L. C. Sloan, 1999: Simulating the water balance of the Aral Sea with a coupled regional climate-lake model. *J. Geophys. Res.,* **104,** 6583–6602.

Song, Y., F. H. M. Semazzi, L. Xie, and L. J. Ogallo, 2004: A coupled regional climate model for the Lake Victoria basin of east Africa. *Int. J. Climatol.,* **24,** 57–75.

Stewart, R. E., and Coauthors, 1998: The Mackenzie GEWEX Study: The water and energy cycles of a major North American river basin. *Bull. Amer. Meteor. Soc.,* **79,** 2665–2683.